PHYSICAL REVIEW B VOLUME 48, NUMBER 4 15 JULY 1993-II

Finite-temperature properties of sodium clusters

Nengjiu Ju and Aurel Bulgac
National Superconducting Cyclotron Laboratory and Department of Physics and Astronomy, Michigan State University, East Lansing, Michigan 48824-1321
(Received 7 December 1992; revised manuscript received 9 March 1993)

We present geometric and energetic properties of sodium clusters with 8, 14, 20, 30, and 40 atoms using an effective many-body interaction among sodium atoms in the framework of an improved isothermal molecular-dynamics approach. These clusters undergo two phase transitions and the two transition temperatures increase with the cluster size. These phase transitions are the equivalents of bulk melting and of boiling in a finite system. However, finite particle effects are particularly strong. These clusters show a more pronounced thermal expansion than the bulk, with significant nonlinear effects. Both the shape and size change rather dramatically with the temperature and the ionic degrees of freedom give a dominating contribution to the entropy, thus effectively controlling the thermal behavior of these clusters.

I. INTRODUCTORY REMARKS

There are several reasons why it is interesting to study finite-temperature properties of atomic clusters, in particular of simple metal clusters. Most of the theoretical studies are performed at zero temperature, while most of the experimental results obtained so far are for relatively hot clusters[1,2] and it is very likely that these clusters are melted. On the other hand, the properties of finite systems at nonzero temperatures are of unquestionable theoretical interest,[3] in particular because of the presence of phase transitions in these finite systems.[4] The relative role of the surface versus volume effects is significantly enhanced in atomic clusters in comparison with the bulk. Since the ion cores are so much heavier than the electrons and the physical phenomena of interest occur in a region where the ionic density of states is extremely high,[5] a classical description of the ions seems more than reasonable. One the other hand, a quantum description of the electronic degrees of freedom is supported by the experimental evidence of pure quantum phenomena, reminiscent of the similar nuclear phenomena.[1,2]

In this paper we attempt to elucidate to some extent the role of a finite temperature in sodium clusters. The approach chosen by us is not irreproachable and for that reason some justification is appropriate. One can distinguish roughly two dominant trends in the literature: (i) pure adiabatic picture with an explicit treatment of the ionic degrees of freedom, which can be subdivided in two subclasses (ia) explicit treatment of the electronic degrees of freedom and (ib) implicit treatment of the electrons via an effective many-body classical potential for the ions; and (ii) featureless ionic background and explicit finite-temperature treatment of the electronic degrees of freedom. We shall not discuss here the quantum-chemistry calculations, which because of their rather ambitious goal, are limited to relatively small clusters.[6]

The approach (ia) seems to be accepted as the most "fundamental" way to describe atomic clusters at zero as well as at finite temperatures.[7] It amounts to a classical description of the ionic degrees of freedom—which seems to be a very reasonable approximation, with the exception of very light atoms such as H, He, and to some extent Li—and a density-functional theory within the local-density approximation (DFT-LDA) for electrons, augmented with a pseudopotential interaction between ionic cores and valence electrons.[7–9] From the point of view of a pure practitioner, the main drawback of this type of approach is the appalling amount of computer time required to extract relevant physical information. It is for this reason that several groups decided to simplify the treatment of the electronic degrees of freedom by using relatively old ideas, originated in condensed-matter physics, such as the tight-binding approximation (see Ref. 10 for a sample of references), embedded atom,[11] etc. The "natural" extension of these methods to finite temperatures still does raise some questions. Although one can accept this type of approach for the description of insulators, where the gap between the occupied and unoccupied electronic states is sufficiently large and the assumption that the electrons are at all times essentially at zero temperature seems reasonable, the applicability of the strict adiabatic approximation for metals or atomic metallic clusters is questionable. One possible approach seems to be the generalization of the DFT-LDA to finite temperatures.[12] However, this line of thought implies a relatively quick relaxation of the electronic degrees of freedom. At low temperatures the relaxation times in many-fermionic systems have a $1/T^2$ behavior[13] and ionic and electronic relaxation times can become comparable. Moreover, atomic clusters are likely rather floppy objects and level-crossing phenomena can occur. In such a case nonadiabatic effects could prove to be quite important and in any event this seems to be yet a *terra incognita.*

A further simplification (ib) relies on the use of an effective many-body interaction among atoms, derived as

 ©1993 The American Physical Society

before in the Born-Oppenheimer approximation for the electrons.[2,14–16] In particular, the strongly delocalized character of the valence electrons in simple metallic systems is at the origin of the many-body character of this effective potential and it cannot be simulated by two-body forces only. In this way one loses some pure quantum features, such as shell effects, odd-even effects, etc. However, one has the advantage, like in a Thomas-Fermi approximation, of describing the gross properties of the clusters, since volume and surface effects seem to be mimicked rather well by this type of model.[15]

The last listed type of approach, (ii), emphasizes solely the role of electrons, while the ionic degrees of freedom form a simple featureless jellium background, without any dynamic or thermodynamic properties.[1,2,17,18] The main *raison d'être* for such models is the hypothesis that the electron dynamics dominates completely the properties of simple metallic clusters, as manifested in abundances, odd-even effects, electromagnetic and optical properties, supershell effects, etc. While perfectly suited to explain this range of phenomena, the jellium approach has its own inherent limitations, especially when finite-temperature properties of metallic clusters are concerned. The gross properties of metallic clusters are rather poorly described in such pure electronic models. For example, the volume energy (total energy per particle) derived in a jellium model is about 2.26 eV (Ref. 17) as contrasted with the cohesive energy for sodium 1.113 eV. This fact alone sheds strong doubts on the treatment of the ions as a physically featureless background. In the pure jellium model the shape and stability of a cluster are totally governed by the electronic degrees of freedom. If the volume energy is so strongly affected by the ions, a similar strong effect for the surface tension, due to the ionic degrees of freedom, is plausible.

Moreover, a large series of molecular-dynamics (MD) calculations[2,4] point to the existence of a large number of isomers, which are absent in a pure jellium description, and their presence gives rise to the phase transitions occurring in atomic clusters. The phase space for the ionic degrees of freedom increases with increase of temperature/excitation energy at a much faster rate than the phase space for the electrons. Since the electrons behave essentially like a degenerate Fermi gas, one can estimate the electronic density of states using Bethe's Fermi gas formula[19]

$$\rho_{\rm el}(E) = \frac{\exp\left[\sqrt{\pi^2 N E/\varepsilon_F}\right]}{\sqrt{48E}}, \tag{1}$$

where N is the number of valence (delocalized) electrons in the cluster, ε_F is their Fermi energy, and E is the electronic excitation energy. For the ionic degrees of freedom an estimate from below (see Sec. III) for their density of states can be obtained from the classical formula for $3N-6$ intrinsic degrees of freedom in the harmonic approximation (Debye model)[5]

$$\rho_{\rm ion}(E) = \frac{E^{3N-7}}{(3N-6)!}\prod_{i=1}^{3N-6}\frac{1}{\omega_i}, \tag{2}$$

where N is the number of atoms in the cluster and ω_i are the vibrational frequencies of the normal modes. For the Na_{20} cluster one obtains in this way $\rho_{\rm el} \approx 4\times 10^4$ eV^{-1} and $\rho_{\rm ion} \approx 10^{58}$ eV^{-1} at an excitation energy of 3 eV. Consequently, the finite-temperature properties, the phase transitions in particular, should be dominated by the ionic degrees of freedom. Since the density of states is directly linked with the entropy, one can rephrase the above discussion in terms of entropic effects; the electronic entropy is much smaller than the ionic entropy.

Experimentally, sodium clusters are likely produced in a liquid state, with an estimated temperature around a few hundred degrees. This could serve as an explanation of the spectacular success of the jellium model. Being in a liquid state, the ions are rather mobile and therefore the cluster can be easily deformed. If the contribution to the surface tension, originating from the ionic degrees of freedom, is significantly smaller than the electronic part, one can expect that the electronic degrees of freedom (through the quantum shell effects) would play the major role in determining the shape and the stability of the cluster. The surface energy for liquid bulk sodium ($\sigma = [0.699 - 3.18\times 10^{-4}(T - T_{\rm melting})]$ eV) (Ref. 20) seems to be in qualitative agreement with the value extracted from jellium calculations, $\sigma_{\rm jellium}(T = 400$ K$)=0.5918$ eV.[18(a)] (The total surface energy is defined as $\sigma N^{2/3}$, where N is the number of atoms in the cluster.) However, the surface tension for liquid bulk sodium shows a relatively strong temperature dependence, while the jellium model[18(a)] seems to underestimate it by at least one order of magnitude in the temperature range $T = 0$–600 K, $d\sigma_{\rm jellium}/dT \approx 2$–$8\times 10^{-5}$ eV/K compared to 3.18×10^{-4} eV/K for liquid bulk sodium.[20] This comparison seems to indicate that a combined treatment of the ionic and electronic degrees of freedom is desirable in order to understand the finite-temperature properties of these clusters. The apparent agreement between the jellium prediction and the bulk value for the surface tension might very easily prove to be an accident.

MD calculations with effective many-body potentials definitely fail to describe the electronic shell effects. The amplitude of the so-called shell-correction terms (computed in the spherical approximation, which overestimates them as a result) never exceeds 1–3 eV for clusters with up to a few hundred atoms and a little bit more for larger ones.[2,18(a)] When converted into energy per atom, the magnitude of the shell corrections is relatively small, about 0.025 eV or 300 K for $N = 40$ (note, however, that this is still about 20% of the potential internal energy for Na_{40} around $T = 500$ K, see Sec. III, and therefore a quite sizable correction). However, as was shown in Ref. 18(b) allowing for the quadrupole and hexadecapole deformations of the clusters, the magnitude of the shell corrections are at most 0.3 eV or so for sodium clusters with up to 50 atoms, i.e., almost an order of magnitude less than estimated in Ref. 18(a). For larger clusters the contribution from these pure quantum effects becomes even smaller, smaller than, or at least of the same order of magnitude as, the uncertainty of the estimated temperatures of the clusters. Nevertheless, the rather fine details of the abundance distributions seem to correlate

qualitatively well with the effects predicted on the basis of the shell corrections.[18,21] One might therefore conclude that, if one is not interested in rather fine details, a pure MD approach to these metallic clusters might provide a quite reasonable description.

Using the arguments of Kubo, Gorkov, and Eliashberg, see reviews,[22] one can show that for temperatures of interest in sodium clusters, the ionic contribution to the specific heat is dominant, since $C_{\rm ion} \geq (3N-6) \gg C_{\rm el}$ (see Refs. 23 and Sec. III). Consequently, the structural changes (phase transitions) are likely to be caused by the ionic degrees of freedom, which is another way of comparing the role of electronic and ionic densities of states.

In spite of all these semiquantitative or qualitative arguments which we have presented in favor of dealing with mostly the ionic degrees of freedom in metallic clusters at finite temperatures, we do not mean to imply that the electronic degrees of freedom are unimportant. On the contrary, we believe that a combined treatment of both ionic and electronic degrees of freedom is warranted. In Ref. 9 such a problem has been studied to a certain extent, however, from those results one cannot make a judgement concerning the relative role of different degrees of freedom. The quite ambitious method chosen there (DFT-LDA in conjunction with the Carr-Parinello method), aimed at a complete description of the system, did not allow the authors to clearly disentangle the specific role played by ions and electrons. The relatively delicate interplay between these two types of degrees of freedom is likely to lead to interesting phenomena; some of them we have partially alluded to above (part of which seem to be beyond the present formulation of DFT at finite temperatures). Even though in the present paper we shall focus by default on the role of the ionic degrees of freedom, we plan to extend our studies in the near future to a comprehensive treatment of all degrees of freedom in these clusters.

In the following section we shall formulate explicitly our approach. In particular, we shall present an improved isothermal molecular-dynamics scheme, based on a previous development[24] of the Nosé-Hoover method.[25] Section III is devoted to the presentation of our results, followed by a summary.

II. EQUATIONS OF MOTION AND ISOTHERMAL DYNAMICS

The delocalized character of the valence s electrons makes the alkali-metal clusters quite different from noble-gas clusters. In the case of argon clusters one need only introduce an effective two-body interaction among the atoms, typically the Lennard-Jones potential. Electron delocalization makes a two-body interaction among alkali-metal atoms physically unacceptable. Instead of treating the electrons explicitly we shall use a phenomenological interaction: the many-body alloy potential.[2,14–16]

The Hamiltonian describing the properties of a sodium cluster used by us is

$$H = E_{\rm kin} + V = \sum_{i=1}^{N} \frac{\mathbf{p}_i^2}{2m} + V \, .$$

V is a many-body alloy potential of the form

$$V = \frac{E_{\rm coh}}{(1-q/p)\sqrt{Z_b}} \sum_{i=1}^{N} \left\{ \sqrt{\sum_{\substack{j=1 \\ j\neq i}}^{N} \exp\left[-2q\left(\frac{r_{ij}}{r_0}-1\right)\right]} - \frac{q}{p\sqrt{Z_b}} \sum_{\substack{j=1 \\ j\neq i}}^{N} \exp\left[-p\left(\frac{r_{ij}}{r_0}-1\right)\right] \right\} . \tag{3}$$

The first term describes the attractive part of the interaction, due to the hybridization of the valence electrons, and has a many-body character. It is based on the second moment approximation for the electronic density of states at the site i and the assumption that the effective hopping integrals are isotropic, which is fulfilled in the case of sodium. The second term describes the closed-shell repulsion between sodium ionic cores, which can be decomposed into pairwise interactions. For sodium we use $E_{\rm coh} = -1.113$ eV for the bulk cohesive energy, $Z_b = 10.4$ for the effective coordination number in the bulk, $q = 3$ and $p = 9$ for the distance dependence of the hopping integrals and the repulsive interactions, and $r_0 = 3.66$ Å for the bulk equilibrium nearest neighbor distance. For these particular values of the parameters, this interaction describes successfully the energy and the elastic properties of the bcc bulk phase, as well as the bond contraction and energy changes at surfaces.[15]

Since we are interested in the thermal behavior of the clusters, we have to introduce the coupling to a thermal bath. In a recent study of Na_{7-9} clusters,[23] a cubic coupling scheme suggested previously[24] was used. This scheme was an efficient algorithm to achieve ergodicity and also to allow a relatively fast exploration of the phase space.[26] It works well for small clusters such as Na_{7-9}, but the cubic term introduced in the equations of motion makes the integration of the equations of motion rather difficult at high temperatures and for large clusters, since it requires a relatively small time step. For example, the choice of the time step ranged from 2.0×10^{-15} to 0.15×10^{-15} sec for different temperatures in the study of Na_{7-9} clusters.[23] Another drawback of the cubic coupling scheme is that the optimal coupling coefficients are different for different temperatures and clusters.[23] This situation can be quite annoying, especially in the case of relatively large clusters. In this paper, we propose a coupling scheme similar to the one proposed for the description of a Brownian particle.[27] We will make the dependence of the coupling coefficients on the temperature and cluster size explicit. Furthermore, we can use the same integration time step for all cluster sizes and temperatures. In all our simulations, we used 1×10^{-15}

sec as the time step and the simulations were carried out for 10^6 steps. Consequently the system was evolved for 1×10^{-9} sec for all temperatures. This makes the length of the simulation about 7 times longer than in the previous study[23] at high temperatures.

Our coupling scheme to a thermal bath at temperature T is described by the following equations of motion for the coordinates x_i, momenta p_{xi}, and pseudofriction coefficients ξ_x, ζ_x, and ϵ_x (here for the x components only)

$$\dot{x}_i = \frac{p_{xi}}{m}, \tag{4}$$

$$\dot{p}_{xi} = -\frac{\partial V}{\partial x_i} - \frac{\alpha e_0}{NL_0}\xi_x^3 \frac{p_{xi}}{p_0} - \frac{\beta e_0}{NL_0}\zeta_x \left(\frac{p_{xi}^2}{p_0^2} - a_0\right) - \frac{\gamma e_0}{NL_0}\epsilon_x \frac{p_{xi}^3}{p_0^3}, \tag{5}$$

$$\dot{\xi}_x = \frac{\alpha T}{p_0 L_0}\left(\frac{\sum_{i=1}^{N} p_{xi}^2}{NmT} - 1\right), \tag{6}$$

$$\dot{\zeta}_x = \frac{\beta T}{p_0 L_0}\left(\frac{\sum_{i=1}^{N} p_{xi}^3}{NmTp_0} - a_0 \frac{\sum_{i=1}^{N} p_{xi} p_0}{NmT} - \frac{2\sum_{i=1}^{N} p_{xi}}{Np_0}\right), \tag{7}$$

$$\dot{\epsilon}_x = \frac{\gamma T}{p_0 L_0}\left(\frac{\sum_{i=1}^{N} p_{xi}^4}{NmTp_0^2} - \frac{3\sum_{i=1}^{N} p_{xi}^2}{Np_0^2}\right). \tag{8}$$

Similar equations hold for the y and z components. In the equations above, $e_0 \sim mL_0^2\nu_D^2$ is a constant with the dimension of energy, of the order of the energy corresponding to the highest frequency in the system (one can call it the Debye frequency $\omega_D = 2\pi\nu_D$ for a cluster). L_0 is a constant with the dimension of length of order ~ 1 Å, $p_0 = \sqrt{2mT}$ is the average thermal momentum at temperature T, and a_0 is a dimensionless constant of order one. α, β, and γ are dimensionless constants, cluster independent, and their temperature dependence is given by

$$\alpha \sim \beta \sim \gamma \sim \sqrt{\frac{mL_0^2}{Nt_0^2 T}}, \tag{9}$$

where t_0 is the smallest characteristic time scale of the system, i.e., $t_0 \sim 2\pi/\omega_D$. In relation (9) the number of particles N appears explicitly because the amplitude of fluctuations of the terms in parentheses in Eqs. (6)–(8) is proportional to $\sqrt{N}$. All the constants, whose magnitude we have specified only by the order of magnitude, can be varied within reasonable limits, without critically affecting the quality of the simulation. However, relatively large variations of these constants might require significantly longer simulation times. This might not affect the ergodic properties of the equations of motion, and therefore in theory will lead to correct results, provided that the simulation is long enough.

A few clarifications, concerning the nature of this type of coupling to a thermostat, are in order. A complex system is always characterized by a rather wide range of characteristic frequencies (modes). In isothermal MD the thermostat is coupled mostly to some modes. In a three-dimensional system the density of modes is largest at high frequency, like in the phonon density in a solid. Consequently, in order to have the most effective coupling to a thermostat, the characteristic frequencies of the thermostat should be comparable with the Debye frequency of the system under study. An analysis of the above equations of motion shows that this is indeed the case. A quick thermalization implies also that energy is exchanged at a reasonable rate among all the modes of the system (i.e., relatively small apparent relaxation times). At the same time the thermalization of the slowest modes of the system is achieved only if the total time of the simulation is larger than the characteristic time of these slow modes and the intrinsic relaxation times of the system. It is possible to devise an isothermal MD in which coupling to all modes (both slow and fast) is achieved by a slight generalization of the type of couplings studied so far.[28] One may wonder as well why we have introduced a relatively large number of pseudofriction coefficients. Our experience[24,26,27] shows that by increasing the number of pseudofriction coefficients one can ensure a more efficient exploration rate of the system phase space (smaller apparent relaxation times) and hence avoid problems with lack of ergodicity. In particular one can achieve a better convergence in the case of phase transitions when the so-called critical slowing down phenomenon sets in.[26] Moreover, in the case of isolated systems one wants to make sure that there are no conserved quantities (whose presence signals the absence of ergodicity), in particular neither the total angular momentum nor its direction is a constant of motion. The price one has to pay, the increased number of differential equations to be solved, is insignificant, especially for large systems. At the same time, a quicker decorrelation time among the generated phase space configurations (which is *the* essential element of any ensemble average procedure) ensures a much better overall quality of the simulation. This Brownian type of coupling to a thermal bath has a few advantages over the usual Nosé-Hoover type of coupling[25] or its generalizations introduced previously.[24,26] The ergodic properties of the Nosé-Hoover coupling depend very strongly on whether the forces are strong enough and nonlinear. In particular, this type of coupling completely fails to be ergodic for a free system or for harmonic oscillators. At relatively high temperatures, when the system undergoes thermal expansion, some particles spend considerable periods of time without interacting with other particles and as a result the algorithm is (partially) not ergodic. By

judiciously choosing the coupling to thermal bath, the present algorithm is ergodic even for one free particle and as a result for all cluster sizes as well and its ergodic properties become thus independent of the character of the interaction.

Provided that the equations of motion generate ergodic trajectories, one can replace the phase space average by the time average, which is much simpler to compute

$$\langle A(p,q)\rangle = \frac{1}{Z(T)}\int d^{3N}p d^{3N}q \exp\left[-\frac{H(p,q)}{T}\right] A(p,q) = \lim_{t_0\to\infty}\frac{1}{t_0}\int_0^{t_0} dt A[p(t),q(t)], \quad (10)$$

where p,q stand for the momenta and coordinates, $Z(T)$ is the partition function, and $A(p,q)$ is an arbitrary observable.

In this coupling scheme, both the center-of-mass coordinate and momentum of the cluster are not constants of motion. When we discuss the thermal properties below, we will refer everything to the instantaneous center of mass of the cluster and present only the intrinsic thermodynamic properties of the cluster. In order to avoid evaporation at high T (around and above the "boiling" phase transition), we have added a linear restoring force every time a particular interparticle distance $r_{ij} > 3R$, where $R = r_0 N^{1/3}$ and N is the number of particles in the cluster.

III. THERMAL PROPERTIES OF SODIUM CLUSTERS

We shall follow Refs. 4 and 23 to classify the cluster characteristics into two categories: thermodynamic properties (internal energy, specific heat, density of states, phase transitions) and geometric properties (shape, rms radius, momenta of inertia, relative bond length). The energetics and geometry of the cluster are strongly correlated and their analysis is extremely helpful in understanding the thermal behavior of atomic clusters.

A. Thermodynamic properties

During each time step we have monitored the kinetic, potential, rotational, vibrational, and total energies of the cluster. The total kinetic energy carries no useful information about a system in the canonical ensemble and we have used it merely as a check of the quality of our simulation. However, the kinetic energy of a cluster can be separated in an unique way into two nontrivial parts, rotational and vibrational energies.[29] Although one might expect that the rotational energy could be different from that of a rigid body, since the clusters are to some extent floppy objects, in the whole range of temperatures studied we have found that these clusters behave essentially like rigid bodies. In particular the rotational specific heat of the clusters is $C_{\rm rot} = 3/2$ as for a rigid body. This is due to the fact that in this temperature range the thermal rotational motion is not fast enough to lead to any significant centrifugal stretching.

The only pertinent physical information comes from the analysis of the potential energy of the clusters. For each temperature, we bin the value of the potential energy at each time step, and construct the histogram $f(E_{\rm pot},T)$. This distribution of the potential energy at a given temperature T is

$$f(E_{\rm pot},T) = \frac{1}{Z_{\rm pot}(T)}\rho(E_{\rm pot})\exp\left(-\frac{E_{\rm pot}}{T}\right), \quad (11)$$

where $\rho(E_{\rm pot})$ is the density of states originating from the potential energy only, and

$$Z_{\rm pot}(T) = \int \rho(E_{\rm pot})\exp\left(-\frac{E_{\rm pot}}{T}\right) dE_{\rm pot} \quad (12)$$

is the potential-energy partition function. The distribution $f(E_{\rm pot},T)$ is peaked near the average potential energy for the corresponding T, and drops off rapidly on both sides. This allows for a reconstruction of the density of states over an energy range comparable to the width of $f(E_{\rm pot},T)$.[23,30] By piecing together parts of $\rho(E_{\rm pot})$ from simulations at different temperatures one can reconstruct the density of states over a significant energy interval, up to an undetermined multiplicative factor, which can in principle be determined as well. The logarithm of the densities of states of the potential energy for the clusters studied are shown in Fig. 1 along with the logarithm of the corresponding Debye density of states, Eq. (2), divided by $(3N-8)/2$. One can clearly see an increased density of states at higher excitation energies, which we associate with the softening of the clusters and which leads to the onset of the phase transitions. The internal energy and the specific heat can be determined from the following standard relations:

$$U(T) = \langle E_{\rm pot}\rangle = \frac{1}{Z(T)}\int E_{\rm pot}\rho(E_{\rm pot})\exp\left(-\frac{E_{\rm pot}}{T}\right) dE_{\rm pot}, \quad (13)$$

$$C(T) = \frac{\langle E_{\rm pot}^2\rangle - \langle E_{\rm pot}\rangle^2}{T^2}, \quad (14)$$

once the density of states is known. We have computed these quantities using the above relations and checked them also against the corresponding averaged quantities obtained during each separate simulation, and the agreement between the two methods was satisfactory. However, in spite of the fact that our simulation time is rather long (1 nsec), the temperature dependence of some quantities is often not very smooth and some fluctuations are still present (their magnitude will be evident in some of the quantities presented in the following subsection, for which an equivalent of the density of states cannot be defined). This is indicative of the fact that even longer simulation times and/or an optimization of the coupling scheme to the thermostat are needed. The extracted density of states proved to be a rather smooth function of the energy (the inherent statistical fluctuations, due to finite simulation times, are indistinguish-

able in the plots). The internal energies presented here are calculated with respect to the ground-state energy of each cluster. The temperature dependences of the internal energy and of the specific heat are displayed in Figs. 2 and 3. Even though the change in the slope as a function of temperature is not so evident for $U(T)$, one can clearly identify the existence of two phase transitions in Fig. 3. The lowest phase transition can be associated with the melting and the highest one with the boiling of the cluster. As expected, in finite systems the phase transitions are not sharp and not as well defined as in an infinite system. However, one can unmistakably conclude that "something quite dramatic happened" to the cluster. As the cluster size increases, the two phase transitions become better defined and in the thermodynamic limit they will likely correspond to the melting and boiling phase transitions for bulk sodium, with $T_{\rm melting} = 371$ K and $T_{\rm boiling} = 1156$ K. The reason for the appearance of these phase transitions is the dependence of the density of states on the excitation energy of the cluster. At low excitation energies, below the melting point, the density of states has a power-law behavior, characteristic for an ensemble of harmonic oscillators; see Eq. (2). The cluster resembles a small crystal and the atoms perform only small amplitude oscillations near their equilibrium positions. This is reminiscent of the Einstein model for a solid. Note, however, that the finite number of ionic degrees of freedom leads to a finite number of vibration energies. Once the excitation energy is increased, the power-law behavior changes to an exponential one, see Fig. 1, the available phase space increases at a tremendous rate, and as a result so does the entropy of the cluster. At approximately $0.4\times N$ eV excitation energy, the density of states for the cluster exceeds the Debye density of states, see Eq. (2), by about $(3N-6)/2$ orders of magnitude. The logarithm of the density of states is essentially the entropy of the system $[S(E) = \ln\rho(E)]$. Our results show that at this excitation energy the entropy per particle exceeds the Debye model estimate by approximately 3–4 units. One can see that the two transition temperatures go up with the cluster size and both melting and boiling occur at lower temperatures in a cluster than in the bulk.[2,4] In finite systems these temperatures are obviously not sharply defined and both melting and boiling occur in a range of temperatures. A cluster has a significant part of its atoms (or perhaps better to say, most of them) at the surface. These atoms are not strongly bound, since their mean coordination number is lower than that for the inner atoms, and it is relatively easy to "shake them up." For that reason atomic clusters "below the melting point" are in a rather unusual state, sometimes called the glassy, the molten, or the fluctuat-

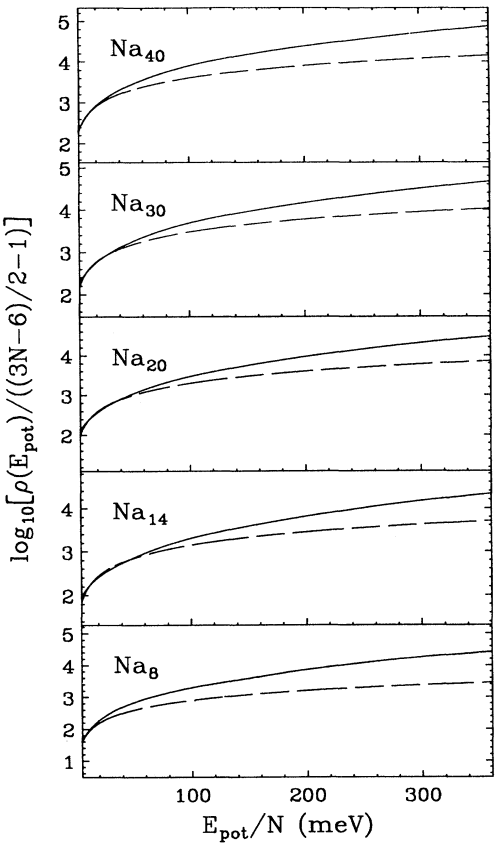

FIG. 1. The decimal logarithm of the unnormalized density of states (potential energy only) as a function of the excitation energy per particle (solid line) and the Debye model expectation (dashed line), divided by $(3N-8)/2$.

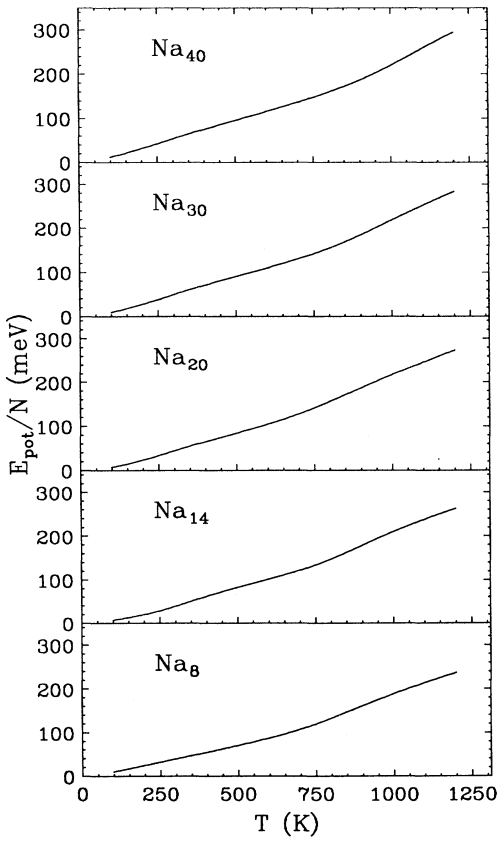

FIG. 2. The temperature dependences of internal potential energies per particle, $U(T)/N$.

ing state.[2,16,23,31] "Above the melting point" they start behaving like liquids, as one can see more easily in the behavior of their pair-correlation function (see the next subsection and Ref. 23).

As a side remark, we would like to stress the advantage of performing an MD calculation in the canonical rather than microcanonical ensemble. One finds often in the literature the statement that the two approaches are essentially equivalent with respect to the amount of physical information extracted and for that reason different authors rather often prefer microcanonical simulations to canonical ones. In a canonical simulation one can relatively easily extract the density of states, which is unaccessible in a microcanonical one, and the thermodynamic behavior of the system can be easily inferred and understood. For a finite system, the density of states plays a similar central role as in statistical physics of large or infinite systems. In particular, it is much less expensive to perform a canonical MD and find structural isomers than in a straightforward search. If an isomer exists, its presence will show up at sufficiently high temperatures, as, in particular, a more careful analysis of the behavior of the density of states shows. (To some extent a similar ideology is behind the popular simulated annealing method.)

In spite of the fact that we are dealing here with such small systems, we decided to estimate the latent heat of fusion for sodium from these simulations. Since the first phase transition occurs around 200–300 K, and the transition peak is very broad, we will simply take 500 K as the temperature at which we regard the clusters are completely in a liquid state. If there is no phase transition, the potential internal energy at temperature T would be $(3N-6)T/2$, as for pure harmonic oscillators (note that the ionic degrees of freedom are treated classically). We shall identify the excess over the internal energy of pure oscillators as the energy necessary to melt the cluster, i.e., the energy needed to cause a structural change of the system. We estimate the heat of fusion to be a value between 2.36 and 3.45 kJ/mole, which compares unexpectedly well with the value 2.6 kJ/mole for bulk sodium.[20] One can try to estimate in the same manner the heat of vaporization as well. At high temperatures the quality of our simulations is worse, due to significant evaporation. Nevertheless, we obtain a value which is approximately equal to the experimentally measured heat of vaporization for sodium 89.6 kJ/mol (within 15–20%). This is not very surprising, since the effective interaction we are using has the correct asymptotic behavior of the cohesive energy for large systems built in, and the heat of vaporization is almost equal to it.

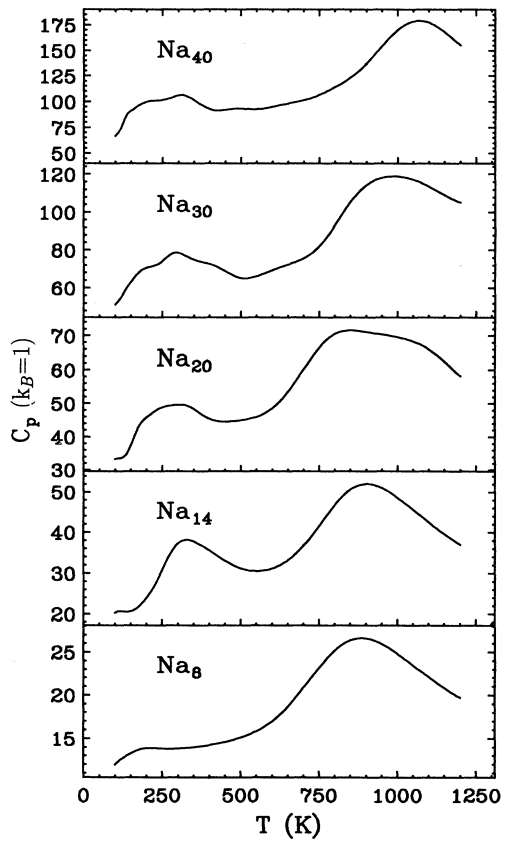

FIG. 3. The temperature dependences of the potential-energy contribution to the specific heat.

B. Geometric properties

A very sensitive indicator of structural changes in a cluster is the rms relative bond length[4,23]

$$\delta = \frac{2}{N(N-1)} \sum_{i<j}^{N} \frac{\sqrt{\langle r_{ij}^2 \rangle - \langle r_{ij} \rangle^2}}{\langle r_{ij} \rangle}. \tag{15}$$

The temperature dependence of the rms relative bond length is shown in Fig. 4. As we have mentioned above, at low temperatures, "below the first phase transition," the cluster behaves like a small crystal, with the atoms oscillating with small amplitudes around their equilibrium positions. At temperatures around 200 K the atoms are at their equilibrium positions for relatively long periods of time. However, from time to time an atom jumps from one equilibrium position to another due to thermal fluctuations.[2,23] The rms relative bond length changes drastically around this temperature, indicative of a structural change. At still higher temperatures, the atoms become extremely mobile and move across the entire cluster.[23] In the region of the second phase transition 850–1000 K, we observe a second increase in δ. This is partially linked with the fact that some atoms can evaporate, even though at a not very significant rate yet. At temperatures above 1000 K, the evaporation of atoms is significant and the precision of our results is therefore reduced. A better approach will be a grand canonical ensemble at these temperatures, suited for the description of the liquid-vapor coexistence. The structural transition in these sodium clusters can be seen also in the behavior of the (unnormalized) pair correlation function $f(r_{ij})$; see Fig. 5. Below the first phase transition the interparticle separations are rather well defined, as one would expect for a small crystallite. In the fluid phase, even though

one can see a well-defined short-range correlation among particles, the long correlation is almost completely lost and at very high temperatures the presence of the vapor phase is obvious.

For each spatial configuration of the cluster, we have calculated three geometric quantities: the rms radius of the cluster, which characterizes the cluster size; the shape parameter β, for the degree of asphericity of the cluster; and the shape parameter γ ($0 \leq \gamma \leq \pi/3$), which describes the triaxiality of the cluster.[23] These parameters provide an average information about the size and shape of the clusters. The rms radius and shape parameters β and γ are related to the principal momenta of inertia ($I_1 \geq I_2 \geq I_3 \geq 0$) through the following relations:

$$I_k = \frac{2}{3} r^2 \left[1 + \beta \sin\left(\gamma + \frac{(4k-3)\pi}{6}\right)\right], \quad k = 1, 2, 3, \tag{16}$$

where

$$r = \sqrt{\frac{1}{N}\sum_{i=1}^{N} \mathbf{r}_i^2} \quad \left(\sum_{i=1}^{N} \mathbf{r}_i = 0\right) \tag{17}$$

is the rms radius of the matter distribution. The condition that the semiminor axis of the associated ellipsoid of the inertia is positive

$$a^2 = \frac{r^2}{3}[1 - 2\beta \sin(\gamma + \pi/6)] \geq 0. \tag{18}$$

$\gamma = 0$, then $I_1 = I_2 > I_3$, and the shape of the cluster is an axially symmetric prolate ellipsoid (cigar) with $0 \leq \beta \leq 1$. For $\gamma = \pi/3$, $I_1 > I_2 = I_3$ and the shape corresponds to an axially symmetric oblate ellipsoid (pancake) and $0 \leq \beta \leq 1/2$. For all the remaining angles in between, the shape is a triaxial ellipsoid. For $\beta = 1/2$ and $\gamma = \pi/3$ the shape is a disk of zero thickness, while $\beta = 1$ and $\gamma = 0$ correspond to a linear chain. The region of allowed values for β and γ has the shape of a triangle in the plane where β is the radial distance and γ is the angle at origin; see Fig. 6.

The temperature dependence of the average principal momenta of inertia and their relative covariances are displayed in Figs. 7 and 8 and the rms radius of the cluster r, and the shape parameters β, γ along with their corresponding covariances, are displayed in Figs. 9–11. From these plots, one can see that all these clusters tend to acquire a cigarlike shape at high temperatures. This might seem a bit peculiar, but is quite easy to understand. One can show that the shape space measure is proportional to $\beta^4 \sin 3\gamma d\beta d\gamma$.[32] Consequently shapes with small val-

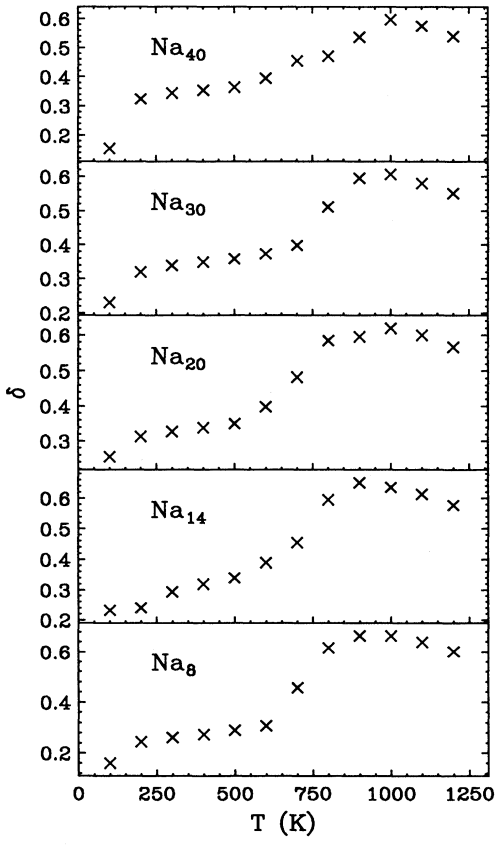

FIG. 4. The temperature dependences of the relative bond length δ.

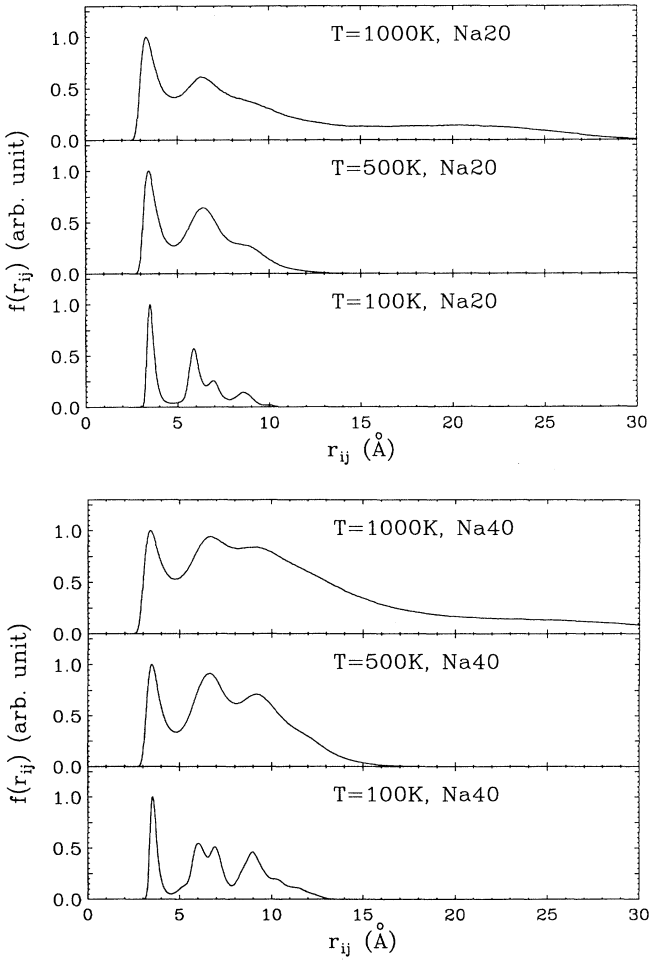

FIG. 5. The pair-correlation function for Na_{20} and Na_{40} at several temperatures.

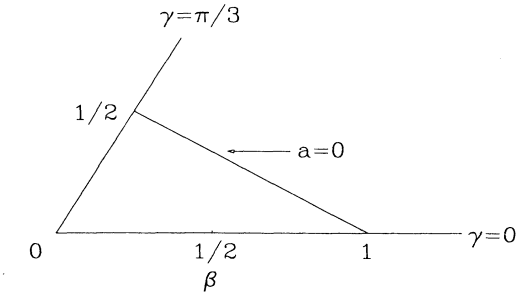

FIG. 6. The allowed region for the shape variables β and γ.

ues of β are strongly suppressed and for the same reason pure oblate or prolate shapes are suppressed as well. At the same time the shapes with as large values as possible for β are strongly favored by this measure and for this reason prolatelike shapes (for which large values of β, $1/2 \leq \beta \leq 1$, $0 \leq \gamma \leq \pi/6$ are possible) start dominating at high temperatures. For $0 \leq \beta \leq 1/2$ oblatelike ($\pi/6 \leq \gamma \leq \pi/3$) and prolatelike ($0 \leq \gamma \leq \pi/6$) shapes are equally probable, according to the shape measure only. One has to keep in mind that these distributions reflect the shape of the free energy of the cluster in the shape space, which takes into account both energetic and entropy properties of the system (the shape space measure is already included). We could have defolded the shape measure from these plots (this is the adopted convention in nuclear physics calculations of deformed nuclei[2,32]), but since any average will involve this measure anyway, such a way of displaying the shape properties of the cluster seems to us to a certain extent misleading. At low temperatures, these clusters are almost incompressible (their rms radii have relatively sharp distributions), but at the same time they can change their shape rather easily (the distributions for both β and γ have significant widths). At high temperatures, these clusters become apparently soft as well, having the characteristics of a compressible fluid. This apparent softness is to some extent an indirect indication of the presence of the vapor. In spite of the shape differences of their ground geometries, the high-temperature behavior of their shapes is quite similar. The character of the shape parameters distributions changes dramatically in the vicinity of the phase transitions. The smallest principal momentum of inertia has the largest fluctuations, since atoms evaporate more readily from the sides of the cigar for obvious reasons (more chances).

We have tried to extract the coefficient of thermal expansion from our results. Unfortunately we did not have enough statistics for a precise determination of the linear and quadratic expansion coefficients. Nevertheless,

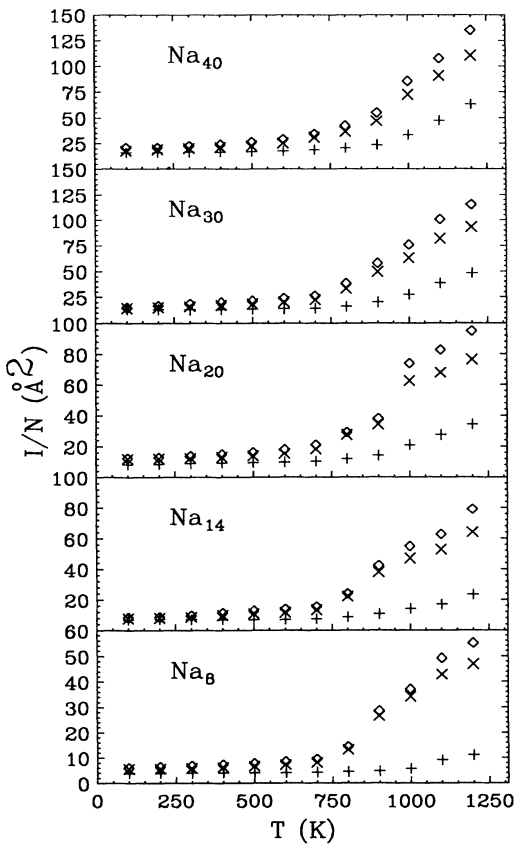

FIG. 7. The temperature dependences of the average principal momenta of inertia per particle.

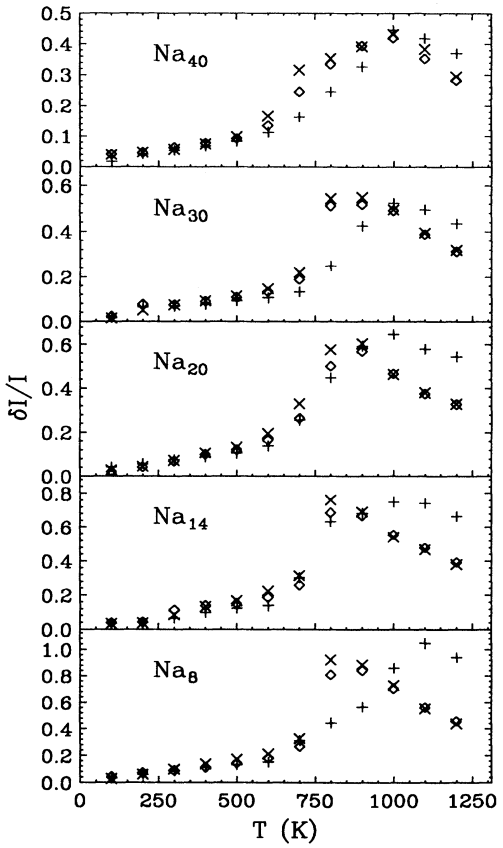

FIG. 8. The temperature dependences of the relative covariances of the average principal momenta of inertia.

as one sees from Fig. 9 the clusters display a rather well-defined nonlinear thermal expansion. This fact might play a quite significant role in explaining the red shift of the Mie plasmon in sodium clusters.[1] In the jellium calculations, routinely used in describing the optical response of sodium clusters, the bulk density for the jellium is assumed. Besides melting and boiling in a quite different way than the bulk, sodium clusters seem to have also a rather distinct thermal expansion behavior. Since the experiments are likely performed with liquid clusters, their larger volume can easily serve as an argument in favor of a lower plasmon energy. The classical Mie plasmon frequency will change approximately as $\delta\omega_{\rm Mie}/\omega_{\rm Mie} = -3\delta r/2r$ when the radius of the cluster changes. At 400–600 K (the estimated temperature of the clusters in nozzle experiments) the linear dimensions of a cluster seem to be about 6–15 % larger than at $T = 0$ K (and significantly larger for higher temperatures), already of the right order of magnitude to explain the observed redshift of the Mie plasmon. At the same time, at these temperatures the volume distribution of the clusters have a quite sizeable width $\Delta r/r \approx 0.04$–0.07 (and significantly larger at higher temperatures), which can explain at least part of the width of the plasmon. In Fig. 12 we present the spherical part of the ionic density, extracted from our simulations at several selected temperatures. [The relatively large fluctuations of $\rho(r)$ near the origin are due to obvious volume effects; near $r \approx 0$ the probability of finding an ion at a distance r from the center of mass of the cluster is proportional to $r^2\rho(r)$ and correspondingly the statistics is lower.] With increasing temperature this density becomes flatter. The radius of the cluster does not seem to vary significantly; however, the surface diffuseness is greatly increased after the first phase transition, which explains the thermal behavior of the rms radius discussed above. This relatively large apparent surface diffuseness is partially due to the fact that the cluster is rather strongly deformed as well. One can conclude that the anomalous thermal expansion of sodium clusters, when compared to the bulk, is mainly due to these surface effects.

An additional contribution to the width of the Mie plasmon in sodium clusters at finite temperatures will arise from shape fluctuations. The rough estimates we presented here should be looked upon only as order of magnitude effects. The shape of the cluster in its ground state and that with one Mie plasmon excited can be quite different and the ultimate shape and width of the plasmon should be estimated using a more detailed procedure.[33]

A comment concerning the potential use of such distributions in jellium-type calculations is in order. These distributions represent ensemble averages. The time scales for the ionic degrees of freedom are significantly lower

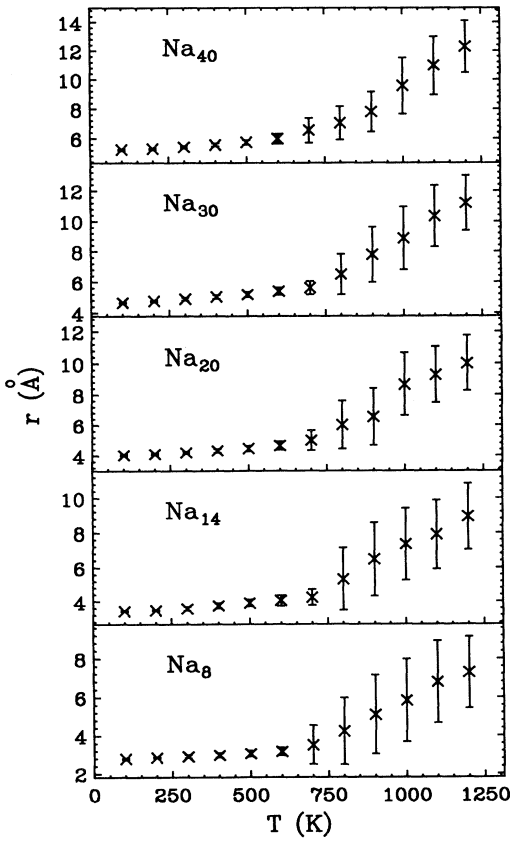

FIG. 9. The temperature dependences of the rms radius and its covariance (error bars).

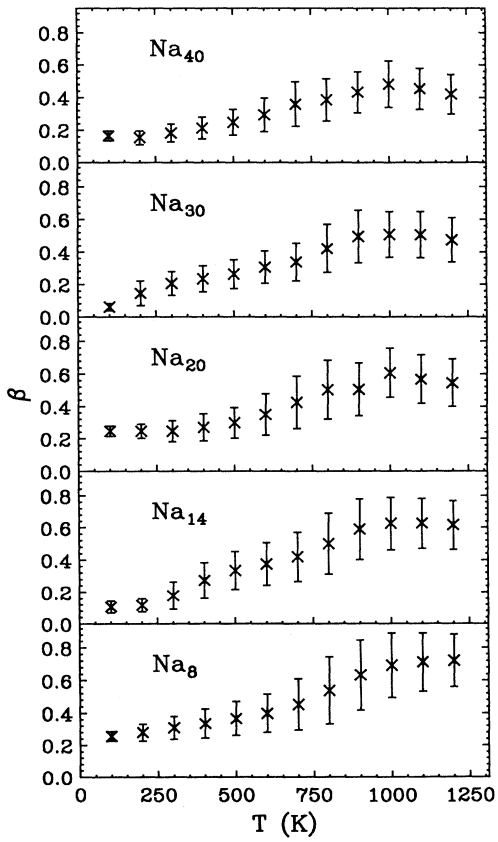

FIG. 10. The temperature dependences of the shape parameter β and its covariance (error bars).

than for the electronic degrees of freedom. If one would like to include such thermal effects in the calculations of the electronic properties and optical response of a cluster, one should perform the corresponding jellium calculations for one member of the ensemble at a time and take the ensemble average only afterwards. In particular, spill-out of the electron density can be more pronounced for some members of the ensemble.

IV. CLOSING REMARKS

Since the energy scale characteristic for the ionic degrees of freedom is relatively small, a huge phase space becomes available upon increasing the temperature of the cluster. These entropic effects show up in rather drastic structural changes and, without being extremely pedantic concerning the adequacy of the terminology, one can characterize these changes as phase transitions in finite systems. With increasing temperature, the clusters go first through a glassy/molten or fluctuating state (200–300 K) and eventually become totally liquid (above 300 K). In this temperature range they are almost incompressible, but highly deformable. At still higher temperatures (850–1000 K) they start boiling, vaporization sets in, and they become rather soft/compressible. In contradistinction with noble-gas clusters,[4] the melting and boiling do not seem to be a geometric or particle number effect and the same behavior is observed for all the clusters we have studied (N = 7, 8, 9, 14, 20, 30, and 40).[23] The thermal expansion properties of these clusters seem to be more pronounced when compared to the bulk and it is mostly due to an increased surface diffuseness and deformation of the cluster. Thermally induced rotation is never fast enough to lead to any rotationally induced effects and in the temperature range studied, one can safely characterize these sodium clusters as rigid bodies with respect to rotational degrees of freedom. The onset of the new phases can be observed in both thermodynamic and geometric properties of the clusters, which have a strong temperature dependence.

The present approach does not account for the electronic degrees of freedom explicitly and therefore electronic shell effects are not accounted for. We expect, however, that, due to the large ionic entropy effects we observe, similar behavior should be observed in a more complete description of these clusters. The electronic shell effects should be rather important at relatively low

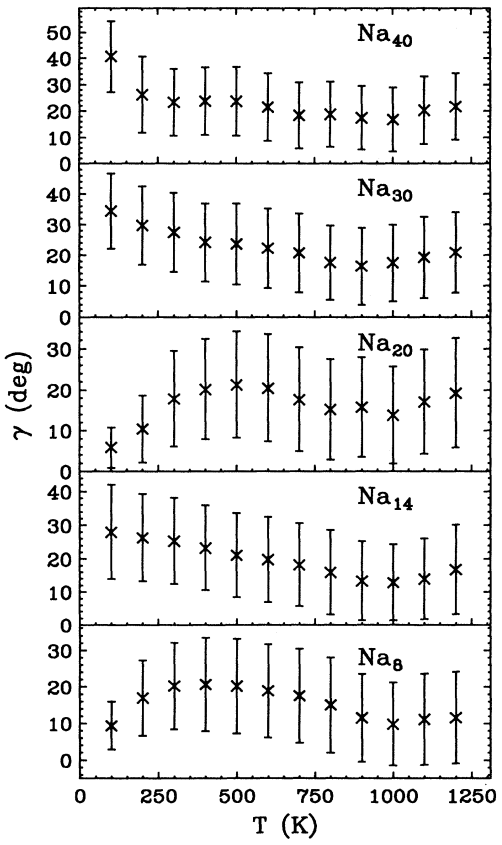

FIG. 11. The temperature dependences of the shape parameter γ and its covariance (error bars).

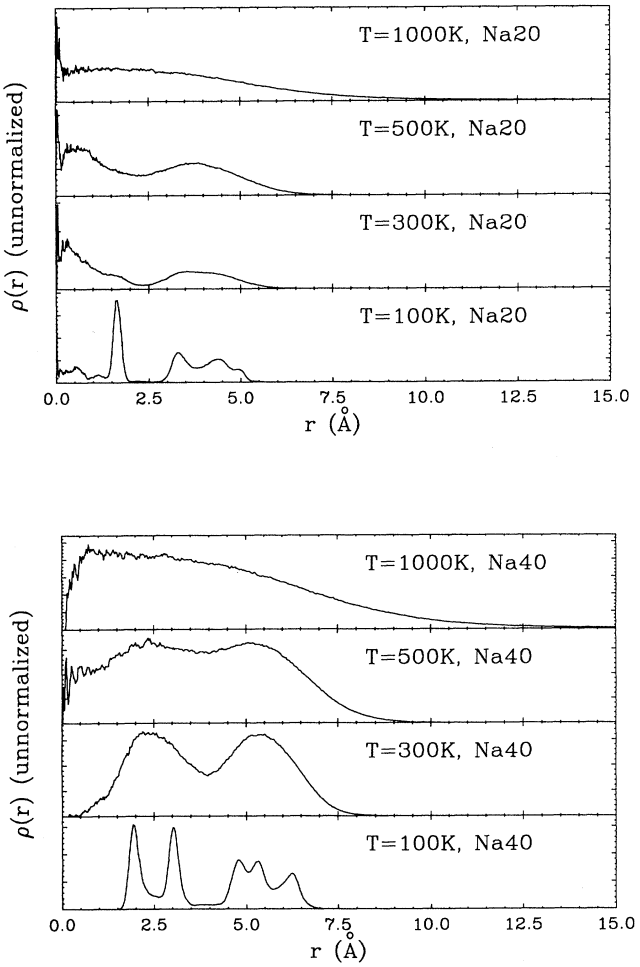

FIG. 12. The extracted spherical part of the radial (unnormalized) ion density distribution for Na_{20} and Na_{40} at several temperatures.

temperatures, below melting. It will be extremely interesting to study the effects of the large geometric fluctuations on the electronic properties and on the optical response in particular (unless in a combined treatment the clusters do not become more stiff, which does not quite seem to happen[9]).

ACKNOWLEDGMENTS

We thank G.F. Bertsch, C. Lewenkopf, B. Mottelson, D. Tománek, and V. Zelevisky for discussions. Support was partially provided under NSF Grants Nos. PHY–8906670, PHY–8920927, and PHY–92091690.

[1]W.A. de Heer, W.D. Knight, M.Y. Chou, and M.L.Cohen, Solid State Phys. **40**, 93 (1987); W.A. de Heer, Rev. Mod. Phys. (to be published).

[2]S. Sugano, *Microcluster Physics* (Springer-Verlag, Berlin, 1991).

[3]T.L. Hill, *Thermodynamics of Small Systems* (Benjamin, New York, 1963, 1964), Pts. 1 and 2.

[4]R.S. Berry, T.L. Beck, H.L. Davis, and J. Jellinek, Adv. Chem. Phys. **70**, 75 (1988); H.L. Davis, J. Jellinek, and R.S. Berry, J. Chem. Phys. **86**, 6456 (1987); R.S. Berry, J. Jellinek, and G. Natanson, Phys. Rev. A **30**, 919 (1984).

[5]G.F. Bertsch and R. A. Broglia, *Oscillations in Finite Quantum Systems* (Cambridge University Press, Cambridge, in press), Chap. 10.

[6]V. Bonačić–Koutecký, P. Fantucci, and J. Kutecký, Chem. Rev. **91**, 1035 (1991).

[7]R.M. Dreizler and E.K.U. Gross, *Density Functional Theory* (Springer-Verlag, Berlin, 1990); M.C. Payne, M.P. Teter, D.C. Allan, T.A. Arias, and J.D. Joannopoulos, Rev. Mod. Phys. **64**, 1045 (1992).

[8]I. Moullet, J.L. Martins, F. Reuse, and J. Buttet, Phys. Rev. Lett. **65**, 476 (1990).

[9]P. Ballone, W. Andreoni, R. Car, and M. Parrinello, Europhys. Lett. **8**, 73 (1989); U. Röthlisberger and W. Andreoni, J. Chem. Phys. **94**, 8129 (1991).

[10]D.J. Chadi and R.M. Martin, Solid State Commun. **19**, 643 (1976); D. Tománek and M.H. Schlüter, Phys. Rev. Lett. **61**, 2331 (1991); L. Goodwin, J. Phys. Condens. Matter **3**, 3869 (1991); R. Poteau and F. Spiegelmann, Phys. Rev. B **45**, 1878 (1992).

[11]J.K. Nørskov and N.D. Lang, Phys. Rev. B **21**, 2131 (1980); J.K.Nørskov, *ibid.* **26**, 2875 (1982).

[12]U. Gupta and A.K. Rajagopal, Phys. Rep. **87**, 259 (1982).

[13]A.A. Abrikosov, L.P. Gorkov, and I.E. Dzyaloshinski, *Methods of Quantum Field Theory in Statistical Physics* (Dover, New York, 1975); D. Pines and P. Nozieres, *The Theory of Quantum Liquids* (Benjamin, New York, 1966). Note, however, that the $1/T^2$ behavior of the fermionic relaxation time is strictly valid for infinite systems and its extrapolation to a finite system should be taken with certain care.

[14]R.P. Gupta, Phys. Rev. B **23**, 6265 (1981).

[15]D. Tománek and K.H. Bennemann, Surf. Sci. **163**, 503 (1985); D. Tománek, S. Mukherjee, and K.H. Bennemann, Phys. Rev. B **28**, 665 (1983); **29**, 1076(E) (1984); D. Tománek, A.A. Aligia, and C.A. Balseiro, *ibid.* **32**, 5051 (1985); W. Zhong, Y.S. Li, and D. Tománek, *ibid.* **44**, 13 053 (1991).

[16]S. Sawada and S. Sugano, Z. Phys. D **14**, 247 (1989); J. Jellinek and I.L. Garzon, *ibid.* **20**, 239 (1991); I.L. Garzon and J. Jellinek, *ibid.* **20**, 235 (1991).

[17]W. Ekardt, Phys. Rev. B **29**, 1558 (1984); **31**, 6360 (1985); D.E. Beck, *ibid.* **30**, 6935 (1984); **35**, 7325 (1985).

[18](a) O. Genzken and M. Brack, Phys. Rev. Lett. **67**, 3286 (1991); (b) S. Frauendorf and V.V. Pashkevich, in Proceedings of the ISSPIC–6 Conference [Z. Phys. D (to be published)].

[19]C.A. Engelbrecht and J.R. Engelbrecht, Ann. Phys. (N.Y.) **207**, 1 (1991).

[20]*CRC Handbook of Chemistry and Physics*, 70th ed. (CRC, Boca Raton, FL, 1990).

[21]J.S. Pedersen, S. Bjornholm, J. Borggreen, K. Hansen, T.P. Martin, and H.D. Rasmussen, Nature **191**, 733 (1991).

[22]W.P. Halperin, Rev. Mod. Phys. **58**, 533 (1986); T.A. Brody, J. Flores, J.B. French, P.A. Mello, A. Pandey, and S.S.M. Wong, *ibid.* **53**, 385 (1981).

[23]A. Bulgac and D. Kusnezov, Phys. Rev. Lett. **68**, 1335 (1992); Phys. Rev. B **45**, 1988 (1992).

[24]A. Bulgac and D. Kusnezov, Phys. Rev. A **42**, 5045 (1990); D. Kusnezov, A. Bulgac, and W. Bauer, Ann. Phys. (N.Y.) **204**, 155 (1990); D. Kusnezov and A. Bulgac, *ibid.* **214**, 180 (1992).

[25]S. Nosé, J. Chem. Phys. **81**, 511 (1984); Mol. Phys. **52**, 255 (1984); Prog. Theor. Phys. Suppl. **103**, 1 (1991); W.G. Hoover, Phys. Rev. A **31**, 1695 (1985); W. G. Hoover, *Molecular Dynamics*, Lecture Notes in Physics Vol. 258 (Springer-Verlag, New York, 1986); W. G. Hoover, *Computational Statistical Mechanics* (Elsevier, Amsterdam, 1991).

[26]J.H. Sloan, D. Kusnezov, and A. Bulgac, *Computational Quantum Physics* (AIP, New York, 1992), Vol. 260, p. 23; J. Sloan, D. Kusnezov, and A. Bulgac, Nucl. Phys. B **26**, 623 (1992); Phys. Lett. B **296**, 379 (1992).

[27]A. Bulgac and D. Kusnezov, Phys. Lett. A **151**, 122 (1990).

[28]A. Bulgac and D. Kusnezov (unpublished).

[29]J. Jellinek and D.H. Li, Phys. Rev. Lett. **62**, 241 (1989).

[30]P. Labastie and R.L. Whetten, Phys. Rev. Lett. **65**, 1567 (1990).

[31]S. Iijima and T. Ichihashi, Phys. Rev. Lett. **56**, 616 (1986); P.M. Ajayan and L.D. Marks, *ibid.* **60**, 585 (1988); **63**, 279 (1989).

[32]A. Bohr and B. Mottelson, *Nuclear Structure* (Benjamin, New York, 1974), Vol. II, Appendix 2.

[33]G.F. Bertsch and D. Tománek, Phys. Rev. B **40**, 2749 (1989); R. Poteau, D. Maynau, J.-P. Daudey, and F. Spiegelmann (unpublished).